



HAL
open science

Towards improving the electroanalytical speciation analysis of indium

Élise Rotureau, Pepita Pla-Vilanova, Josep Galceran, Encarna Companys,
Jose Paulo Pinheiro

► **To cite this version:**

Élise Rotureau, Pepita Pla-Vilanova, Josep Galceran, Encarna Companys, Jose Paulo Pinheiro. Towards improving the electroanalytical speciation analysis of indium. *Analytica Chimica Acta*, 2019, 1052, pp.57-64. 10.1016/j.aca.2018.11.061 . hal-01950315

HAL Id: hal-01950315

<https://hal.science/hal-01950315>

Submitted on 8 Mar 2019

HAL is a multi-disciplinary open access archive for the deposit and dissemination of scientific research documents, whether they are published or not. The documents may come from teaching and research institutions in France or abroad, or from public or private research centers.

L'archive ouverte pluridisciplinaire **HAL**, est destinée au dépôt et à la diffusion de documents scientifiques de niveau recherche, publiés ou non, émanant des établissements d'enseignement et de recherche français ou étrangers, des laboratoires publics ou privés.

1
2
3
4
5
6
7
8
9
10
11
12
13
14
15
16
17
18

Towards improving the electroanalytical speciation analysis of indium

Elise Rotureau^{*,1,2}, Pepita Pla-Vilanova³, Josep Galceran³, Encarna Companys³,
José Paulo Pinheiro^{1,2}

¹ CNRS, LIEC (Laboratoire Interdisciplinaire des Environnements Continentaux), UMR7360,
Vandoeuvre-lès-Nancy F54501, France.

² Université de Lorraine, LIEC, UMR7360, Vandoeuvre-lès-Nancy F54501, France.

³ Departament de Química, Universitat de Lleida and AGROTECNIO, Rovira Roure 191,
25198 Lleida, Catalonia, Spain

Keywords: indium, free metal, AGNES, SCP, electroanalytical techniques, speciation

19 **ABSTRACT**

20 The geochemical fate of indium in natural waters is still poorly understood, while recent
21 studies have pointed out a growing input of this trivalent element in the environment as a
22 result of its utilisation in the manufacturing of high-technology products. Reliable and easy-
23 handling analytical tools for indium speciation analysis is, then, required. In this work, we
24 report the possibility of measuring the total and free indium concentrations in solution using
25 two complementary electroanalytical techniques, SCP (Stripping chronopotentiometry) and
26 AGNES (Absence of Gradients and Nernstian Equilibrium Stripping) implemented with the
27 TMF/RDE (Thin Mercury Film/Rotating Disk Electrode). Nanomolar limits of detection, *i.e.*
28 0.5 nM for SCP and 0.1 nM for AGNES, were obtained for both techniques in the
29 experimental conditions used in this work and can be further improved enduring longer
30 experiment times. We also verified that AGNES was able (i) to provide robust speciation data
31 with the known In-oxalate systems and (ii) to elaborate indium binding isotherms in presence
32 of humic acids extending over 4 decades of free indium concentrations.

33 The development of electroanalytical techniques for indium speciation opens up new routes
34 for using indium as a potential tracer for biogeochemical processes of trivalent elements in
35 aquifers, *e.g.* metal binding to colloidal phases, adsorption onto (bio)surfaces, etc.

36 1. Introduction

37 In the context of extensive expansion of low-carbon energy technologies, indium has been
38 classified by the EU commission as a near-critical metal regarding the risk of supply chain
39 bottlenecks [1]. The principal industrial application of indium worldwide is for producing
40 indium oxide (In_2O_3) and indium tin oxide (ITO) to make electrically conducting transparent
41 thin films, mainly used for liquid crystal displays and photovoltaic cells. The world's indium
42 production has increased tenfold since the nineties [2]. Indium is almost exclusively obtained
43 as a by-product in zinc smelters operating using sphalerite (a zinc sulphide ore mineral).
44 Besides, the potential of indium recyclability is relatively limited [3]. It is now recognized that
45 the steadily increased use of indium for technology applications is leading to a significant
46 anthropogenic input in the biogeochemical cycle of indium [4]. While measured total amounts
47 of indium in freshwaters are usually low *e.g.* ranging from 1 to 15 pM in Japanese rivers [5],
48 more abundant concentrations are found in (i) groundwaters, with reported values of 81 nM
49 and 0.18 μM in Canada [6] and in a polluted site in Taiwan [7], respectively, (ii) acid mine
50 drainage waters, where the amount may reach up to 0.25 μM [8] (iii), soils with measured
51 average values of 0.15 $\mu\text{mol kg}^{-1}$ [9] and (iv) sediments, with measured values ranging from
52 0.13 to 0.87 $\mu\text{mol kg}^{-1}$ [10].

53 In recent years, there is a growing interest in the environmental fate [6,9] and toxicity [11–13]
54 of indium, but they remain mostly unknown [4]. The aqueous geochemistry of indium is very
55 close to other trivalent ions such as gallium and scandium, elements that are all heavily
56 influenced by hydrolysis reactions [14]. In aqueous solution, indium acts as a hard acid which
57 preferentially interacts with ligands containing oxygen donor atoms, *e.g.* hydroxides,
58 carboxylate and phenolate groups. As for other metal cations, the fate of indium will likely be
59 controlled by its interaction with natural organic matter (NOM) and/or with the mineral
60 surfaces, mostly clays or iron hydro-oxides [15]. Since the understanding of metal speciation is

61 considered as a key issue for evaluating the adverse effects of metallic contamination in natural
62 ecosystems and especially in aquifers, and there are growing demands for on-site indium
63 detection, robust and versatile techniques for laboratory set-up need to be urgently developed.
64 To date, analytical determinations of indium in the environment are commonly performed using
65 inductively coupled spectroscopy and atomic absorption spectroscopy preceded usually by a
66 pre-concentration step [4]. Therefore, current efforts are made to conceive new techniques
67 trying to minimize handling steps before the measurement of free or total indium concentrations
68 in aqueous samples. Among them, ion selective electrodes have been successfully designed
69 with organic solid-contact indium sensors reaching the detection threshold of 0.1 μM [16,17].
70 Electroanalytical sensors offer great opportunities to quantify the total indium amount at
71 micromolar concentrations levels, using ex-situ plated antimony film [18–20] or bismuth film
72 [21] electrodes. Another study reported the analytical performance of the adsorptive stripping
73 electrochemical techniques (AdSV) in terms of linear ranges of calibration and limits of
74 detection [22]. Because AdSV requires the addition of a complexing agent, further speciation
75 analyses are more involved. Very recently, the technique Absence of Gradients and Nernstian
76 Equilibrium Stripping (AGNES), commonly used for free ions quantification of trace metal
77 elements [23–25], has been extended to indium analysis with a sensitivity below nanomolar
78 concentrations [26]. This equilibrium technique provides new perspectives for acquiring
79 thermodynamic information pertaining to indium binding properties with molecular or colloidal
80 ligands. As detailed in this pioneering work, the methodology using mercury drop electrodes
81 still necessitates some improvements regarding the measurement reproducibility and the rather
82 long acquisition times which can exceed 30 min [26].

83 In this work, we report the possibility of measuring the total and the free indium concentrations
84 using two complementary electroanalytical techniques. The first one is Stripping
85 chronopotentiometry (SCP) [27] which is used to quantify the total indium amount in the

86 samples, after a preliminary acidification step. SCP is a stripping technique, thus presenting a
87 very low detection limit, typically on the nanomolar level, and furthermore is not affected by
88 the adsorption of organic ligands at the surface of the working electrode [28]. The second
89 technique exploited in this work, AGNES [29] is employed for the direct determination of the
90 free metal concentration, thus providing an estimation of the stability constants of the
91 complexed metal species in solution.

92 This study explores the analytical indium sensing performance and robustness of these two
93 techniques using a thin film mercury electrode (TMFE) deposited on a rotating disk electrode
94 (RDE). The results demonstrate the added advantages of these two techniques *e.g.* their easy
95 handling, high sensitivity (sub-nanomolar detection limits), good reproducibility and ability to
96 perform indium speciation studies.

97

98 **2. Material and methods**

99 *2.1. Reagents and solutions*

100 All solutions were prepared with ultra-pure water (18.2 M Ω cm, Elga labwater). In(III) and
101 Hg(II) solutions were obtained from dilution of a 1000 mg L⁻¹ certified standard solution
102 (Fluka). The ionic strength is set with sodium perchlorate (NaClO₄) (Fluka, >>98%),
103 perchlorate acid (HClO₄) (Fluka) or sodium hydroxide (NaOH) (Merck suprapur) solutions
104 were used to adjust the pH. Nitrogen (>99.999% pure) for the electrochemical experiments was
105 purchased from Air Liquide. Ammonium acetate (NH₄Ac), ammonium thiocyanide (NH₄SCN)
106 and hydrochloric acid (HCl) (all p.a. from Merck) were used to prepare the solution for the
107 cleaning of the working electrode and re-dissolution of the mercury film. Oxalate solution was
108 obtained from solid sodium oxalate (Na₂C₂O₄·2H₂O) from (Fluka, >99.5% pure). The humic
109 substances were extracted following the IHSS procedure for soil organic matter [30] from peat
110 in the Mogi river region of Ribeirão Preto, São Paulo State, Brazil. The elemental analysis

111 yielded C: 51.3%; H: 4.2% and N: 3.8% with an ash content of 0.6%, while potentiometric
112 titrations showed carboxylic and phenolic groups of 3.2 and 3.0 mol kg⁻¹ respectively, well
113 within the usual values for a peat humic acid [31].

114 *2.2.Apparatus*

115 An Ecochemie Autolab type III potentiostat controlled by GPES 4.9 software (Ecochemie, The
116 Netherlands) was used in conjunction with a Metrohm 663VA stand. Dri-ref-5 electrode from
117 WPI (Sarasota, FL, U.S.A.) and a glassy carbon electrode were used as reference and counter
118 electrode, respectively. The working electrode was a thin mercury film (TMF) plated onto a
119 rotating glassy carbon disk of 2 mm diameter (Metrohm) as detailed in section 2.3. The
120 preparation of the rotating disk/thin mercury film electrode (TMF/RDE) was repeated daily for
121 each set of experiments. A 827 pH lab (Metrohm) was used as pH-meter for this study.

122

123 *2.3.Working electrode preparation*

124 The first step consists in polishing the electrode surface using alumina (Metrohm) slurry for 1
125 min, followed by a thorough washing with ultrapure water, then sonicating the electrode in
126 ultrapure water during 1 min.

127 The second step consists in an electrochemical pre-treatment of 50 successive cyclic
128 voltammograms between -0.8 and +0.8 V at 0.1 V s⁻¹ in NH₄Ac 1 M /HCl 0.5 M solution [32].

129 The third step is the electrodeposition of the thin Hg film. So, the glassy carbon was immersed
130 in a Hg(II) solution 0.12 to 0.24 mM (pH 1.9) and deposited using a potential of -1.3 V for a
131 period of time ranging from 240 s to 420 s using a rotation rate of 1000 or 1500 rpm. The
132 different conditions produce electrodes of different thicknesses, thus after each working day,
133 the charge associated with the deposited Hg was determined to assess the state of the mercury
134 film. This was carried out by electronic integration of the linear sweep stripping peak of Hg

135 with a scan rate $\nu = 0.005 \text{ V s}^{-1}$ in 5 mM of ammonium thiocyanide (pH 3.4) using a stripping
136 range from -0.15 V to +0.4 V [25].

137

138 *2.4. Experimental protocol*

139 In the laboratory set-up, a disposable polystyrene cell is placed in a double-walled container
140 connected to a refrigerated-heating circulator and the temperature of the solution is set to 25°C.

141 The solution is initially purged using nitrogen for 15 min and afterwards a nitrogen blanket is
142 always maintained above the sample solution.

143 SCP experimental parameters are as follows: (i) the deposition step is carried out at the specified
144 deposition potential E_d in the limiting current region for a set time, t_d (between 45 and 180 s)
145 using a rotation rate of 1000 rpm (ii) a stripping current, I_s of 3 μA , under non-rotating
146 conditions, is applied until the potential reaches a value well past the reoxidation transition
147 plateau.

148 AGNES measurements were performed following the hereafter detailed protocol. The metal
149 deposition step at the Hg electrode was achieved by applying a potential E_d fixed for a suitable
150 deposition time (t_d) using a rotation rate of 1000 rpm. The magnitude of the potential E_d is
151 chosen in order to accumulate a sufficient amount of indium to be safely quantified, while
152 establishing a situation without concentration gradients in the solution at the vicinity of the
153 electrode surface and Nernstian equilibrium (more details in the section 3 of the supplementary
154 material) within a reasonable time. The gain (or preconcentration factor) Y is the ratio between
155 the concentrations of reduced and oxidised metal at equilibrium. The charge (Q) of the stripping
156 stage (in the variant called AGNES-SCP [33]) was taken as response function. It has been
157 shown that the measured stripping charge is proportional to the free metal concentration, which
158 for indium reads:

$$159 \quad Q = Y \eta_Q [\text{In}^{3+}] \quad (1)$$

160 where $[\text{In}^{3+}]$ is the free indium concentration and η_Q is a proportionality factor that (due to
161 Faraday's law) can be computed from the mercury volume V_{Hg} , as

$$162 \quad \eta_Q = 3 F V_{\text{Hg}} \quad (2)$$

163 where F is the Faraday constant.

164 The experimental protocol for calibration measurements, for both SCP and AGNES, consists
165 of preparing a solution made up from 20 mL of 100 mM NaClO_4 , 60 μL of 1M HClO_4 to fix
166 the pH at 2.5, so as *ca.* 97.4% of indium is in free form, according to Visual Minteq [34] using
167 Birjuk's constants [35]. Then several additions of indium stock solution 10 μM and 100 μM
168 are achieved to construct the calibration plots.

169 The determination of free indium in presence of oxalate was carried out for a total indium
170 concentration of 0.6 μM at pH 3 with various sodium oxalate concentrations *i.e.* 10, 20, 40 and
171 100 μM and at pH 4 with sodium oxalate concentration of 10, 20 and 40 μM .

172

173 *2.5. Quantification of free indium in humic acids suspensions by using AGNES*

174 Batch suspensions of 5 mg L^{-1} purified humic acids stabilized in 100 mM NaClO_4 electrolyte
175 were prepared. Indium concentration was fixed at values in the concentration range of 0.1 μM
176 to 2.5 μM . Then, the pH was fixed at 3.75 by addition of HClO_4 and the solutions were
177 equilibrated at least 24 h prior to the measurements. Before the determination of the free indium
178 concentration, a calibration plot was performed using the AGNES parameters previously
179 mentioned. The batches were disposed in the electrochemical cell and AGNES measurement
180 was repeated three times to determine the free indium concentration.

181 **3. Results and Discussion**

182 *3.1 Total metal determination*

183 The determination of the total concentration of indium by electrochemistry in natural samples
184 needs a previous acidification step to pH values equal or below 2.5 in order to destroy

185 complexes with organic matter or particles and to prevent the formation of indium hydroxides.
186 This is best achieved using HClO_4 , due to the absence of indium perchlorate complexes, which
187 is not the case with nitrate, sulphate [36] or chlorate [14].

188 As mentioned in the introduction, environmental concentrations of indium in natural waters
189 vary from extremely low values in surface waters (picomolar) to relatively high (sub-
190 micromolar) values in polluted groundwater. In soils and sediments, the content per kg lies in
191 a relatively large interval with an average value close to 150 nmol kg^{-1} . Thus, the target
192 detection limit should be as low as possible to account for the surface waters concentrations,
193 while being able at the same time to reach the relatively high concentration values to measure
194 sediment and soil extracts.

195 The detection linearity range obtained with a unique time deposition of 45 s is very large for
196 indium element when using mercury electrodes. As observed in Figure S1 of the supplementary
197 material (section 1), the linearity domain reaches upper concentrations of $30 \text{ }\mu\text{M}$. This high
198 value stems from the extraordinary amalgamation of indium in mercury (up to 57% (w/w)),
199 which is the highest of all metals [37].

200 Regarding the detection limit, the electroanalytical stripping techniques have the potential to
201 reach extremely low values due to the pre-concentration in the deposition step. Observing the
202 equations for SCP (section 2 in supplementary material), SCP key parameters are stripping
203 current (I_s) and deposition time (t_d) in Eq. (S2.3) and electrode area (A) and thickness of the
204 diffusion layer (δ) in Eq. (S2.4).

205 The detection limit in SCP is conditioned by the presence of dissolved oxygen, since it can
206 reoxidise chemically the amalgamated metal. For the TMF/RDE case, this problem may be
207 minimized using relatively large oxidising currents (I_s), thus competing with the chemical
208 oxidation induced by the dissolved oxygen in solution. Our previous experience with
209 performing SCP in TMF/RDE's showed that I_s larger than $10 \text{ }\mu\text{A}$ tends to increase the noise in

210 the signal, so that a trade-off combination of an I_s on the order of 2-5 μA coupled with a
211 reasonable nitrogen purge (usually 15 to 20 minutes) followed by blanketing the system with
212 nitrogen provides the best results in terms of detection limit. Applying values of I_s lower than
213 1 μA demands longer purging times driving the method unsuitable for field conditions.

214 Regarding the electrode area, the commercial electrodes are normally circular with diameters
215 spanning over 2 and 5 mm. This size is constrained by the three electrodes cell configuration
216 used in voltammetry that demands a counter electrode (significantly) larger than the working
217 electrode. Also increasing the electrode area might increase the instrumental noise meaning that
218 the detection limit gain may be marginal.

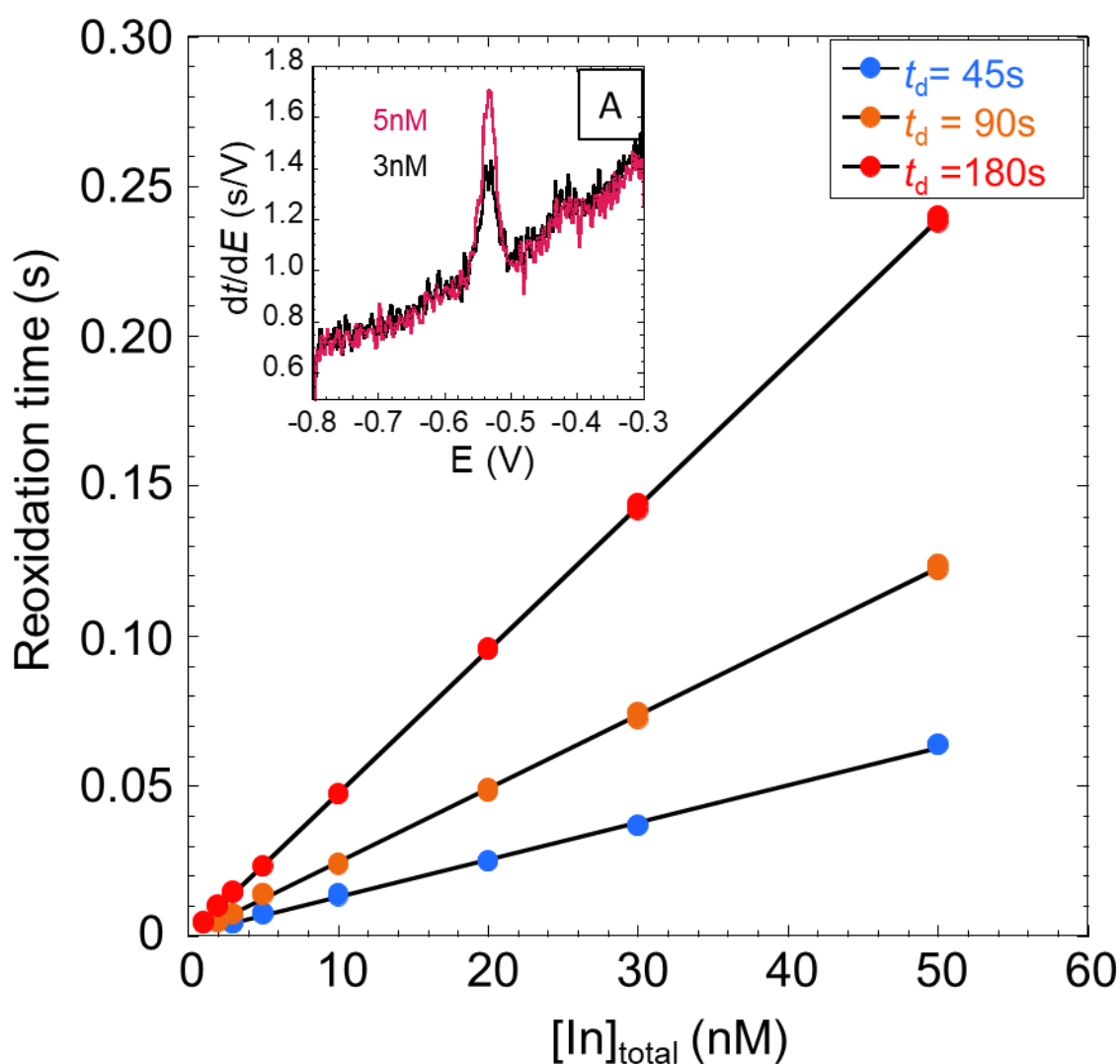
219 The third parameter is the thickness of the diffusion layer (δ) which is dependent on cell
220 geometry and hydrodynamic conditions. In the case of the RDE, increasing the rotation speed
221 will provide better detection limits, however this might impact negatively on the stability of the
222 mercury film. We have observed that the RDE rotation speed should not exceed 1500 rpm to
223 obtain durable electrodes.

224 So, for the parameters discussed above, several constrains define their values leaving only the
225 deposition time (t_d) as a relatively free parameter to obtain better detection limits for total
226 indium determination in acidic media.

227 Figure 1 shows the calibration plots obtained for deposition times 45, 90 and 180 s with
228 TMF/RDE using a rotation speed of 1000 rpm and $E_d = -0.7000\text{V}$, at pH 2.3 in 100 mM NaClO_4 .

229 The calculated detection limits from the standard deviation of residuals ($\text{LOD} = 3s_y/m$ with s_y
230 the standard deviation of the blank response and m the slope of the calibration curve) of the
231 calibration curve for the different deposition times are 21 nM for 45 s, 13 nM for 90 s and 0.5
232 nM for 180 s. According to Eq. (S2.3) of the supplementary material, whenever the oxygen
233 current is negligible in front of I_s , the signal is the product of the deposition time and limiting
234 current, which depends directly on the (total) metal concentration in solution (for a solution

235 with no complexation). Since the LOD is computed using the standard deviation of residuals
 236 and the slope of the calibration plot, it can be reasoned that if the signal is good enough, the
 237 standard deviation of residuals will be reasonably constant, hence the LOD will be inversely
 238 proportional to the slope of the calibration plot. This hypothesis seems to be well confirmed by
 239 the results presented in Figure 1, where a fourfold increase in deposition time (45 s to 180 s)
 240 produced a fourfold decrease in LOD (2 to 0.5 nM). Following this correlation, a LOD of 0.1
 241 nM would require a fivefold increase in deposition time from 180 s to 900 s (15 min).



242
 243 **Figure 1:** SCP calibrations for deposition times of 45 s (blue), 90 s (orange) and 180 s (red), obtained
 244 at $E_d = -0.7000$ V with the TMF/RDE rotation speed 1000 rpm, in 100 mM NaClO₄ medium, pH 2.3.
 245 Inset: SCP curves for indium concentration of 3 and 5 nM for the deposition time of 180 s showing the
 246 signal to noise ratio.

247

248 The inset of Figure 1 depicts two SCP curves for 3 and 5 nM indium giving some insight on the
249 signal to noise ratio. We point out that the signal is the area under the peak and not the peak
250 height.

251

252 3.2 Free metal determination

253 According to Tehrani *et al* [26], the free In^{3+} quantification can be performed using AGNES in
254 a hanging drop mercury electrode (HMDE) which provides a good detection limit. However,
255 they reported repeatability problems and a relatively long analysis time, typically 800 s. To
256 overcome these limitations, we replaced the working HMDE by the TMF/RDE, exhibiting a
257 larger surface to volume ratio, thereby potentially reducing the measurement time [38].

258 From a theoretical point of view, the detection limit for a free metal ion using AGNES depends
259 on the gain (*i.e.* the deposition potential, Eq. (S3.1) of the section 3 of the supplementary
260 material), implying that it effectively depends on the amount of time we are willing to wait until
261 reaching equilibrium. Reasonability constrains these deposition times to less than one hour (a
262 few experimental points per day), and practicality to times up to 10 minutes.

263 With this in mind, we tested AGNES with our TMF/RDE system by carrying out calibration
264 plots for indium in NaClO_4 medium at pH 2.5, initially using deposition potentials roughly in
265 the mid-point of the ancillary Scanning Stripping Chronopotentiometry wave [39] and
266 sufficiently long deposition times to reach equilibrium.

267 A total of 51 calibrations plots were carried out at 10 mM, 30 mM and 100 mM NaClO_4 ionic
268 strength. Repeatability of the calibrations was tested involving three different operators and
269 three voltammetry stands.

270 Table S1 of section 4 in the supplementary material shows that the detection limits (LOD)
271 determined using the standard deviation of residuals of the calibration plot range from a

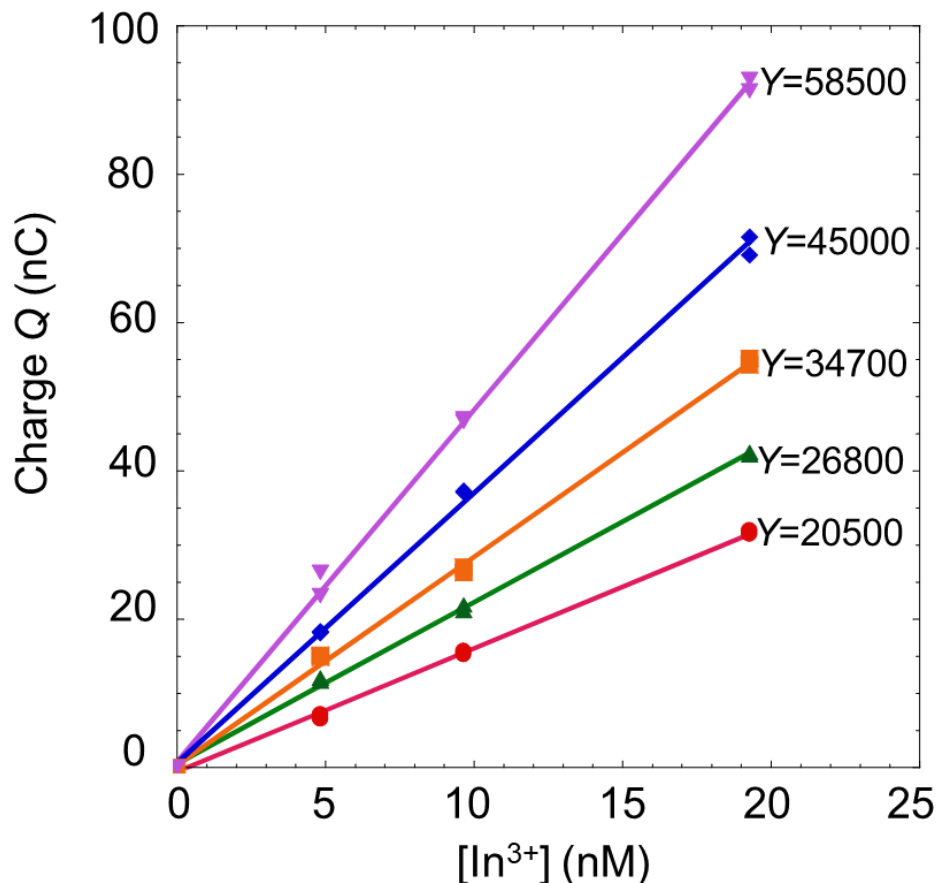
272 minimum of 0.7 nM to a maximum 9.5 nM free indium, depending both on the gain used and
273 the noise of the baseline.

274 The results obtained are repeatable and, during the experimental work, we only discarded one
275 working day, thus demonstrating the robustness of this method. The detection limit obtained in
276 experimental conditions is very satisfactory.

277 The advantage of AGNES is that, by using more negative deposition potentials, the gain (Y)
278 increases, and in turn, the detection limits decreases, provided that a sufficiently long deposition
279 time is applied to guarantee equilibrium.

280 Following Tehrani *et al* [26], the gain (Y_{calib} , associated to the applied potential E_{calib}) is not
281 computed from any ancillary polarographic experiment, but, rather, from the calibration (based
282 on Eq. (3)), once the proportionality factor η_Q is determined from the mercury volume using
283 Eq. (2).

284 Figure 2 shows the calibration plots obtained in 100 mM NaClO₄ at pH 2.6 for different
285 deposition potentials ranging from -0.5850 V to -0.5950 V, where it can be observed that the
286 slope increases significantly corresponding to the calculated gains from 20500 to 58500.



287

288 **Figure 2:** AGNES calibrations at pH 2.6 in 100 mM NaClO₄ medium using different E_d : -0.5850
 289 V, $t_d=180$ s (red dot), -0.5875 V, $t_d=210$ s (green triangle), $E_{calib}=-0.5900$ V, $t_d=240$ s (orange
 290 square), $E_{calib}=-0.5925$ V, $t_d=330$ s (blue diamond) and $E_{calib}=-0.5950$ V, $t_d=390$ s (purple
 291 triangle). Free indium concentration has been computed by Visual Minteq [34] using Biryuk
 292 constant values [35]. The calculated gain (Y) for each calibration plot is reported.
 293

294 In order to reach better detection limits, larger gains than the calibrated ones might be necessary.

295 This can be safely done as long as the measurement corresponds to the same calibration interval

296 for Q and one checks that the equilibrium condition is attained for the pair (deposition

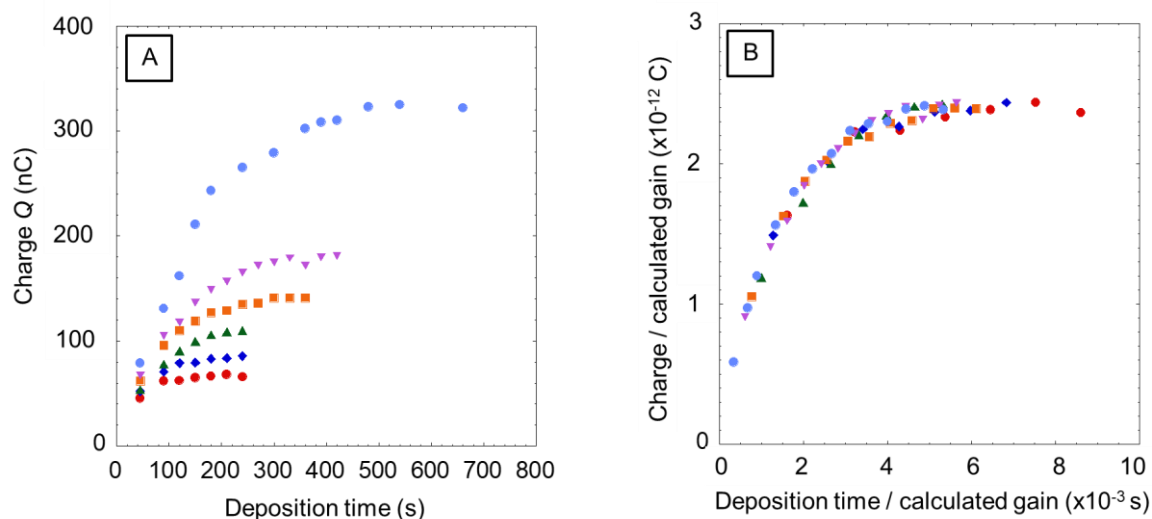
297 potential)/(deposition time). Deposition potentials (E_j) for new gains (Y_j) can be computed

298 taking into account Nernst equation, given the expected linearity of the logarithm of the gain

299 with the deposition potential:

$$300 \quad \ln(Y_j/Y_{calib}) = -\left(\frac{3F}{RT}(E_j - E_{calib})\right) \quad (3)$$

301 To confirm that the equilibrium condition is attained, we performed a series of trajectories
 302 which consist in measuring the accumulated charge in the electrode upon the increase of the
 303 deposition times for given deposition potentials. Figure 3 shows the different trajectories
 304 obtained for 30 nM indium solution in 100 mM NaClO₄ at pH 2.6 obtained for several
 305 deposition potentials indicated in the figure caption. As depicted in Figure 3A, all trajectories
 306 asymptotically tend towards plateau values for sufficiently large deposition time, evidencing
 307 that the equilibrium state is reached after a suitable accumulation stage. The results clearly show
 308 that, for more negative deposition potentials, the equilibrium time is longer and the charge (or
 309 gain) is higher.



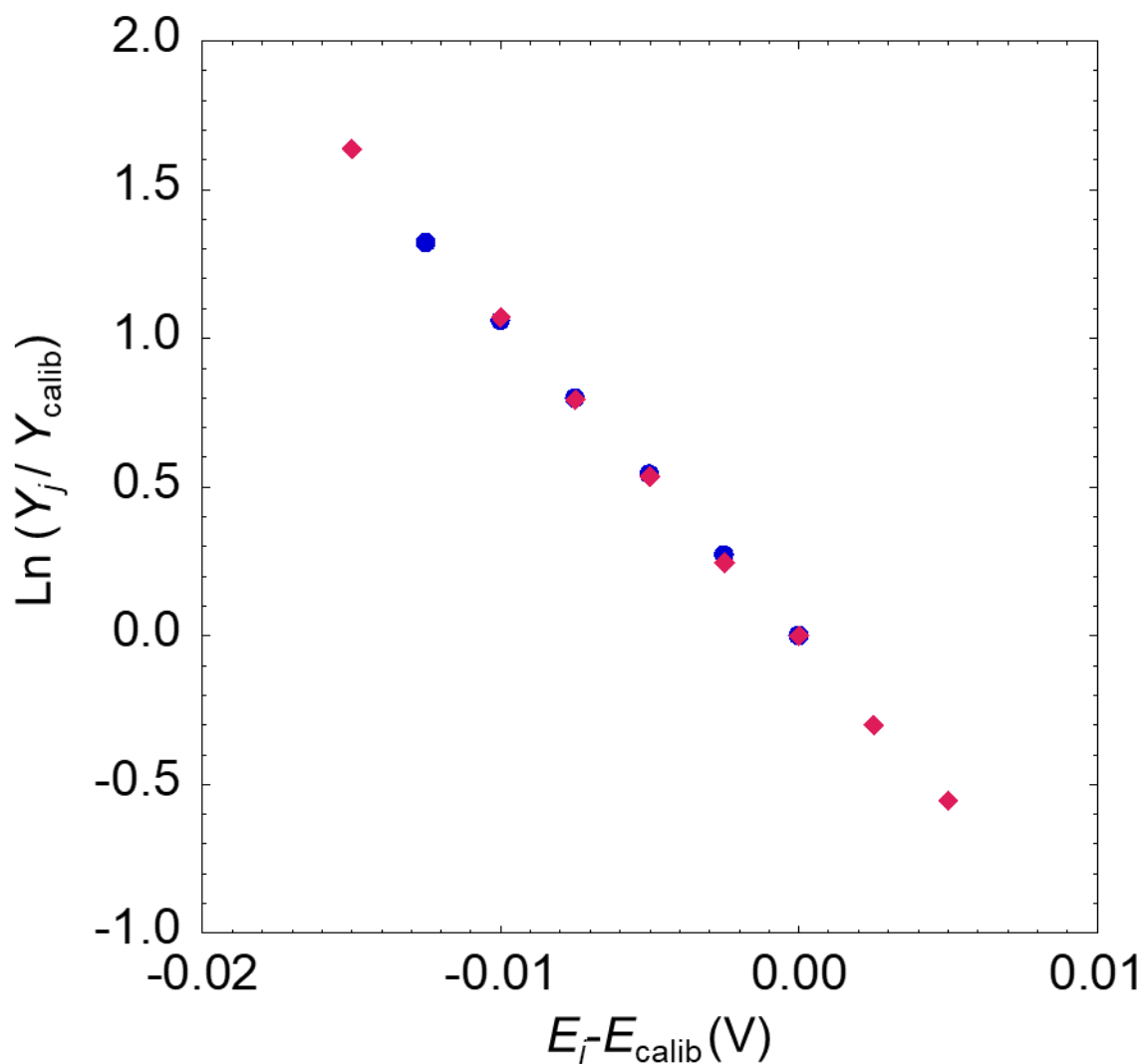
310 **Figure 3:** Experimental trajectories (A) obtained for deposition potentials of -0.5850 V (red dot), -
 311 0.5875 V (blue diamond), -0.5900 V (green triangle), -0.5925 V (orange square), -0.5950 V (purple
 312 triangle) and -0.6000 V (light blue circle) for 30 nM indium concentration in 100 mM NaClO₄, pH 2.6
 313 and for a rotation speed of 1000 rpm, and normalized trajectories (B) by the calculated gain (Y) as a
 314 function of the deposition time over Y .

315
 316 Figure 3B reports the trajectories normalized by the gain as determined from the calibration
 317 plots constructed for each deposition potential. This so-obtained master curve allows an
 318 estimation of the empirical relationship between the equilibrium deposition time and the gain.
 319 Thus, we obtain $t_d = 5 \times 10^{-3} Y$ (s). The proportionality factor is significantly smaller than the value

320 of 10 obtained by Tehrani *et al* [26] using the HMDE, meaning that for a certain gain, the
 321 TMF/RDE will reach equilibrium 2000 times faster than the HMDE.

322 As shown in Figure 4, we validate the Nernstian behaviour of the electrochemical system by
 323 plotting the linear dependence of $\ln(Y_j/Y_{\text{calib}})$ vs. $E_j - E_{\text{calib}}$ (Eq. (3)), according to the
 324 experimentally determined couple (E_{calib} ; Y_{calib}).

325



326
 327

328 **Figure 4:** Dependence of $\ln(Y_j/Y_{\text{calib}})$ according to Eq. (S3.4) for a solution of 30 nM indium in 100
 329 mM NaClO_4 at pH 2.6, with rotation speed 1000 rpm. Different deposition potentials were
 330 employed (blue circle) -0.5825 V, -0.5850 V, -0.5875 V, -0.5900 V, -0.5925 V, -0.5950 V and
 331 (red diamond) -0.5750 V, -0.5775 V, -0.5800 V, -0.5825 V, -0.5850 V, -0.5875 V, -0.5900 V
 332 and -0.5950 V.

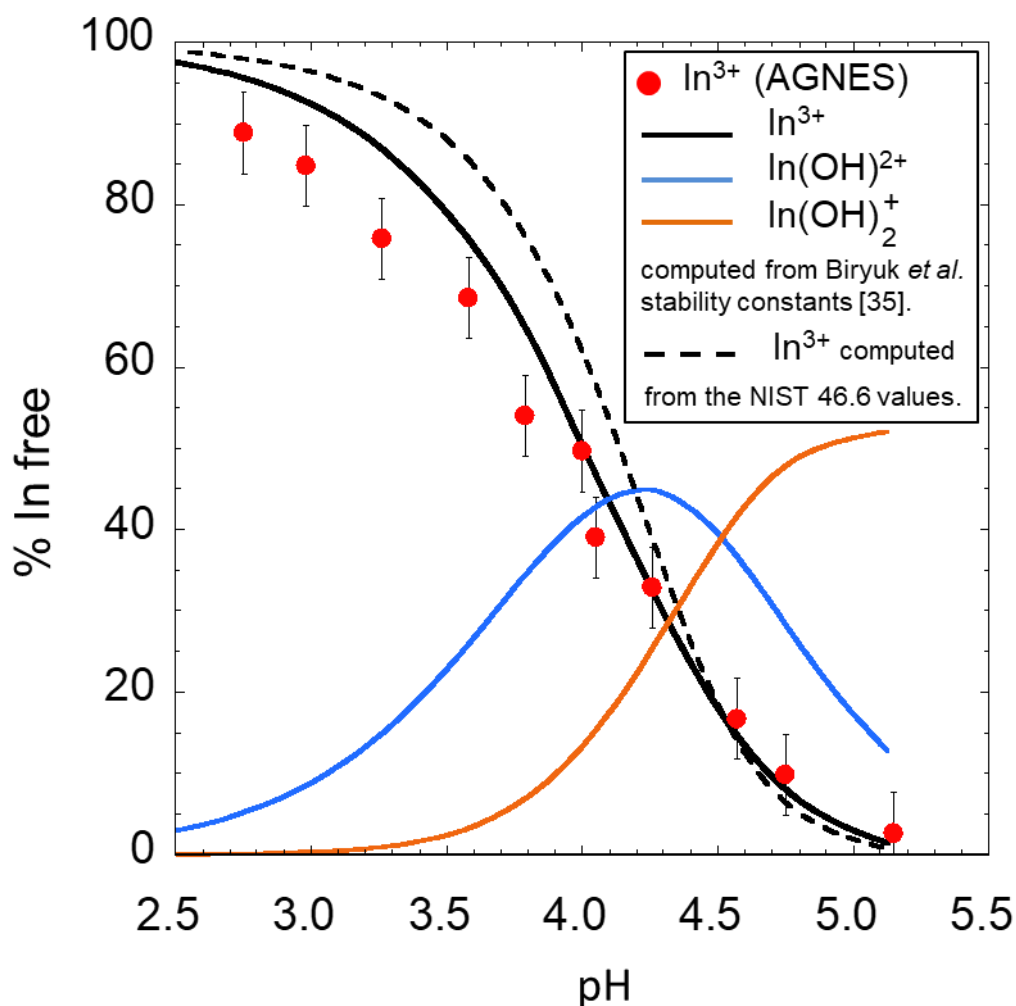
333

334 This Nernstian behaviour is the key to one of the most striking AGNES feature which allows
335 probing a very large range of detection limits, as depicted in Figure 3. The establishment of a
336 calibration at a certain concentration range (for instance from 10 to 300 nM of indium) provides
337 the initial couple (E_{calib} ; Y_{calib}). Then, it is possible to target a relevant gain (Y_j) using Eq. 3
338 derived from Nernst relationship, by applying the calculated E_j . This is particularly helpful in
339 the construction of indium binding isotherms over a wide range of metal coverage of the
340 reactive sites. We will address this feature in detail in the following section for the speciation
341 of indium in presence of complexing ligands.

342

343 3.3 The hydrolysis of indium

344 As for most trivalent metal ions, indium speciation in an aqueous solution is heavily influenced
345 by hydrolysis reactions. AGNES calibration is performed in acidic condition to warrant the
346 predominance of the free form. Although it is expected that no complex species can interfere in
347 the determination of free indium with AGNES, upon pH increase, electrochemically active
348 species $\text{In}(\text{OH})^{2+}$ can help in reaching equilibrium faster [40].



349

350 **Figure 5:** pH dependence of the percentage of free indium in 100 mM NaClO_4 experimentally
 351 determined by the AGNES technique and compared to the thermodynamic speciation of indium
 352 according to the stability constants in [14,35]. The total concentration of indium is 50 μM , $E_d = -0.5800\text{V}$
 353 and $t_d = 120$ s. Error bars are estimated from the relative uncertainties over three AGNES measurements.
 354

355 So, we compared the experimental AGNES results with the thermodynamic speciation
 356 according to Biryuk *et al* [35] and the NIST 46.6 database in the pH range of 2.5 to 5.5. Figure
 357 5 shows a slightly better agreement between the percentages of free ions as determined by
 358 AGNES with those computed by Visual Minteq using the following values of hydrolysis of
 359 In^{3+} $\log K_1 = -3.54$, $\log K_2 = -7.82$ and $\log K_3 = -12.98$ from Biryuk *et al* [35] at infinite dilution. As
 360 expected from its principles, AGNES is measuring the free indium concentration without any
 361 special interference from a possible electroactive $\text{In}(\text{OH})^{2+}$. Indeed, when we reach the

362 equilibrium by the end of the deposition stage of AGNES, In^{3+} is in equilibrium with In^0 , and
363 In^{3+} is in equilibrium with $\text{In}(\text{OH})^{2+}$ (like in the bulk, if we have absence of gradients in the
364 concentrations profiles), so $\text{In}(\text{OH})^{2+}$ should also be in equilibrium with In^0 . The only impact
365 expected from $\text{In}(\text{OH})^{2+}$ being more electroactive than In^{3+} is a contribution from $\text{In}(\text{OH})^{2+}$ to
366 the (transient) accumulation flux, so that the approach to the equilibrium should be faster, but
367 the finally accumulated amount is not influenced by other complexes.

368

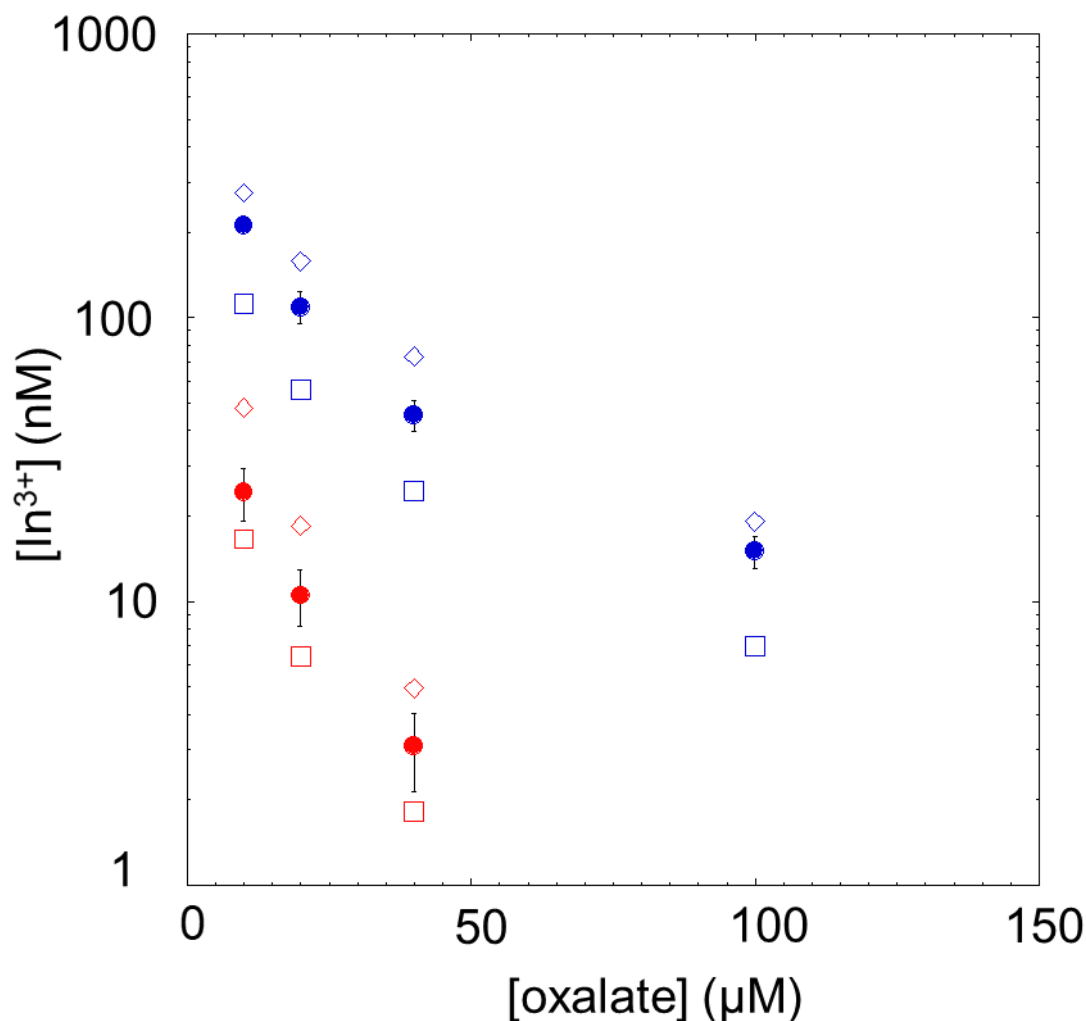
369

370 3.4 Speciation of indium with oxalate and humic acids

371 After establishing that the species measured by AGNES is indeed the free In^{3+} , it is fundamental
372 to evaluate its performance in speciation studies.

373 Figure 6 shows that the results obtained in this study for In-oxalate binding are in reasonable
374 agreement with previously published results, since they lie halfway between the ones reported
375 by Pingarron *et al* [41] and the ones reported by Vasca *et al* [42]. In a previous work using
376 AGNES in the HMDE Tehrani *et al* [26] using somewhat different experimental conditions
377 observed values closer to the ones reported by Vasca *et al* [42]. We must warn that, because of
378 a typing error, the total concentration of indium of $100 \mu\text{mol L}^{-1}$ was unduly reported as $5 \mu\text{mol}$
379 L^{-1} in the caption of figure 6 in [26].

380 We estimated the errors for our AGNES measurements using the 95% confidence interval
381 obtained from the standard deviation of the 4 measurements multiplied by Student factor for
382 binomial distributions ($t_{95,3}=3.182$). As expected, the errors are larger for the smaller values
383 obtained at pH 4, since they are closer to the detection limit.



384

385 **Figure 6:** Free indium concentrations measured by AGNES in presence of increasing
 386 concentrations of oxalate in 100 mM NaClO₄ at pH 3 (blue circle) and pH 4 (red circle). Total
 387 indium concentration is 0.1 μM. The rotation speed is 1000 rpm. Computed values using Visual
 388 Minteq with the stability constants determined by Pingarron *et al* [41] (open diamond) and
 389 Vasca *et al* [42] (open square), and using the Biryuk *et al* [35] constants for the indium
 390 hydroxides complexes.

391

392 One of our main interests in developing these methodologies is the ability to perform indium

393 speciation directly in environmental samples. Since the interaction of indium with natural

394 organic matter (NOM) is expected to be one of the key parameters, about which there is no

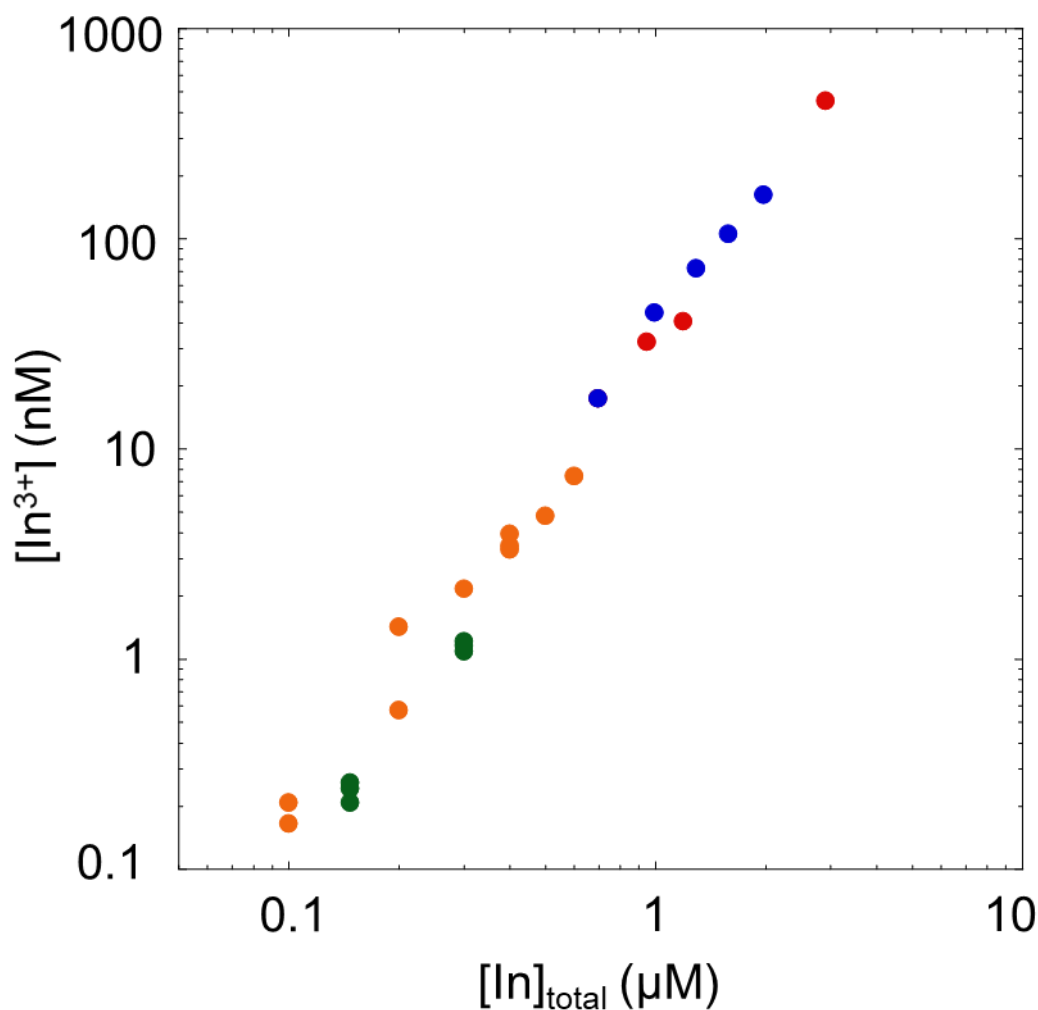
395 information in the literature, we decided to test AGNES in presence of a well-characterised

396 humic sample [31], as a representative colloidal phase in freshwaters.

397 Figure 7 depicts an indium titration of 5 mg L⁻¹ of humic acid substance, at pH 3.75, 100 mM

398 NaClO₄, *i.e.*, the free indium evolution as a function of the total indium concentration added.

399 The orange and green points at very low indium concentration were obtained using the strategy
 400 of changing the deposition potential and computing the new gain using Eq. (3.3). In this
 401 particular case the calibration linked $E_{\text{calib}} = -0.5800\text{V}$ with $Y_{\text{calib}} = 1.6 \times 10^4$, and the new gain
 402 for the experiment in presence of humic acids at $E_d = -0.6300\text{V}$ was $Y = 3.3 \times 10^6$. In this way,
 403 four decades of free indium concentrations are probed by the AGNES technique with
 404 reasonable equilibrium times (less than 10 min). Thus, this methodology opens the way to the
 405 elaboration of indium binding isotherms over a wide range of metal coverage to humic acid
 406 particles. Moreover, we observe a reasonable repeatability amongst the different measurement
 407 (replicates) demonstrating the ability of AGNES to provide robust speciation data.



408
 409 **Figure 7:** Free indium concentrations measured by AGNES in several suspensions of humic acids (5
 410 mg L⁻¹) containing known total indium concentrations, at pH 3.75 and ionic strength of 100 mM NaClO₄.

411 The rotation speed is 1000 rpm. Each colour corresponds to replicates. Error bars estimated from the
412 relative uncertainties over three AGNES measurements, are smaller than points.

413

414

415 **Conclusions**

416 In this work we investigated the ability of two electroanalytical techniques to measure low
417 concentration of total (SCP) and free indium (AGNES). For the total concentration, at pH <2.3,
418 we obtained an excellent detection limit of 0.5 nM for 180 s deposition time.

419 For the free metal determination using AGNES, we demonstrated the enormous saving in
420 experimental time when using the TMF/RDE instead of the HMDE and confirmed the excellent
421 performance of these electrodes in speciation studies, especially when determining extremely
422 low free indium concentrations (down to 10^{-10} M). We also verified that AGNES was able to
423 provide robust speciation data in experiments in presence of humic matter.

424 Due to the absence of trivalent cation complexation data with humic matter, it is our intention
425 to pursue these studies with experiments at different pH values and different ionic strengths,
426 followed by adequate complexation modelling, especially at higher pH values where the
427 influence of indium hydrolysis will be noticeable. Such investigations will open new
428 perspectives for using indium as a powerful tracer of geochemical processes of trivalent
429 elements in terrestrial waters.

430

431 **Acknowledgements**

432 This work has been supported by the French National Research Agency through the national
433 program “Investissements d’avenir” with the reference ANR-10-LABX-21-01 / LABEX
434 RESSOURCES21. We thank the contribution of Jérémy Gloux, Paco Iglesias and Mirella
435 Dammous from University of Lorraine in the preliminary experimental work. Funding from the
436 Spanish Ministry of Economy, Industry and Competitiveness MINECO, project CTM2016-

437 78798 (EC, PPV, JG) is acknowledged. PPV thanks Generalitat de Catalunya for a doctoral FI-
438 AGAUR fellowship.

439

440 **Supplementary material**

441 Section 1: Linearity range for In³⁺ in SCP with TMF/RDE.

442 Section 2: Stripping Chronopotentiometry (SCP) at the TMF/RDE.

443 Section 3: Fundamentals of AGNES.

444 Section 4: Calibration plots obtained with AGNES.

445

446 **AUTHOR INFORMATION**

447 **Corresponding Author**

448 *Email: elise.rotureau@univ-lorraine.fr

449

450 **References**

- 451 [1] European Commission, Critical Metals in the Path towards the Decarbonisation of the EU
452 Energy Sector: Assessing Rare Metals as Supply-Chain Bottlenecks in Low-Carbon
453 Energy Technologies, (2013). [https://ec.europa.eu/jrc/en/publication/eur-scientific-and-technical-research-reports/critical-metals-path-towards-decarbonisation-eu-energy-](https://ec.europa.eu/jrc/en/publication/eur-scientific-and-technical-research-reports/critical-metals-path-towards-decarbonisation-eu-energy-sector-assessing-rare-metals-supply)
454 [sector-assessing-rare-metals-supply](https://ec.europa.eu/jrc/en/publication/eur-scientific-and-technical-research-reports/critical-metals-path-towards-decarbonisation-eu-energy-sector-assessing-rare-metals-supply).
455
- 456 [2] U.S. Geological Survey, 2017, Mineral commodity summaries 2017, (2017).
457 <https://doi.org/10.3133/70180197>.
- 458 [3] L. Ciacci, B.K. Reck, N.T. Nassar, T.E. Graedel, Lost by Design, *Environ. Sci. Technol.*
459 49 (2015) 9443–9451. doi:10.1021/es505515z.
- 460 [4] S.J.O. White, H.F. Hemond, The Anthropiogeochemical Cycle of Indium: A Review of
461 the Natural and Anthropogenic Cycling of Indium in the Environment, *Crit. Rev. Environ.*
462 *Sci. Technol.* 42 (2012) 155–186. doi:10.1080/10643389.2010.498755.
- 463 [5] Y. Nozaki, D. Lerche, D.S. Alibo, M. Tsutsumi, Dissolved indium and rare earth elements
464 in three Japanese rivers and Tokyo Bay: Evidence for anthropogenic Gd and In, *Geochim.*
465 *Cosmochim. Acta.* 64 (2000) 3975–3982. doi:10.1016/S0016-7037(00)00472-5.
- 466 [6] A. Tessier, C. Gobeil, L. Laforte, Reaction rates, depositional history and sources of
467 indium in sediments from Appalachian and Canadian Shield lakes, *Geochim. Cosmochim.*
468 *Acta.* 137 (2014) 48–63. doi:10.1016/j.gca.2014.03.042.
- 469 [7] H.-W. Chen, Gallium, Indium, and Arsenic Pollution of Groundwater from a
470 Semiconductor Manufacturing Area of Taiwan, *Bull. Environ. Contam. Toxicol.* 77
471 (2006) 289–296. doi:10.1007/s00128-006-1062-3.
- 472 [8] S.J.O. White, F.A. Hussain, H.F. Hemond, S.A. Sacco, J.P. Shine, R.L. Runkel, K.
473 Walton-Day, B.A. Kimball, The precipitation of indium at elevated pH in a stream

- 474 influenced by acid mine drainage, *Sci. Total Environ.* 574 (2017) 1484–1491.
475 doi:10.1016/j.scitotenv.2016.08.136.
- 476 [9] A. Ladenberger, A. Demetriades, C. Reimann, M. Birke, M. Sadeghi, J. Uhlback, M.
477 Andersson, E. Jonsson, GEMAS: Indium in agricultural and grazing land soil of Europe -
478 Its source and geochemical distribution patterns, *J. Geochem. Explor.* 154 (2015) 61–80.
479 doi:10.1016/j.gexplo.2014.11.020.
- 480 [10] K. Folens, G. Du Laing, Dispersion and solubility of In, Tl, Ta and Nb in the aquatic
481 environment and intertidal sediments of the Scheldt estuary (Flanders, Belgium),
482 *Chemosphere.* 183 (2017) 401–409. doi:10.1016/j.chemosphere.2017.05.076.
- 483 [11] N.R. Brun, V. Christen, G. Furrer, K. Fent, Indium and Indium Tin Oxide Induce
484 Endoplasmic Reticulum Stress and Oxidative Stress in Zebrafish (*Danio rerio*), *Environ.*
485 *Sci. Technol.* 48 (2014) 11679–11687. doi:10.1021/es5034876.
- 486 [12] C. Zeng, A. Gonzalez-Alvarez, E. Orenstein, J.A. Field, F. Shadman, R. Sierra-Alvarez,
487 Ecotoxicity assessment of ionic As(III), As(V), In(III) and Ga(III) species potentially
488 released from novel III-V semiconductor materials, *Ecotoxicol. Environ. Saf.* 140 (2017)
489 30–36. doi:10.1016/j.ecoenv.2017.02.029.
- 490 [13] C.I. Olivares, J.A. Field, M. Simonich, R.L. Tanguay, R. Sierra-Alvarez, Arsenic (III, V),
491 indium (III), and gallium (III) toxicity to zebrafish embryos using a high-throughput multi-
492 endpoint in vivo developmental and behavioral assay, *Chemosphere.* 148 (2016) 361–368.
493 doi:10.1016/j.chemosphere.2016.01.050.
- 494 [14] S.A. Wood, I.M. Samson, The aqueous geochemistry of gallium, germanium, indium and
495 scandium, *Ore Geol. Rev.* 28 (2006) 57–102. doi:10.1016/j.oregeorev.2003.06.002.
- 496 [15] A. Tessier, C. Gobeil, L. Laforte, Reaction rates, depositional history and sources of
497 indium in sediments from Appalachian and Canadian Shield lakes, *Geochim. Cosmochim.*
498 *Acta.* 137 (2014) 48–63. doi:10.1016/j.gca.2014.03.042.
- 499 [16] V.K. Gupta, A.J. Hamdan, M.K. Pal, Comparative study on 2-amino-1,4-naphthoquinone
500 derived ligands as indium (III) selective PVC-based sensors, *Talanta.* 82 (2010) 44–50.
501 doi:10.1016/j.talanta.2010.03.055.
- 502 [17] M.N. Abbas, H.S. Amer, A Solid-Contact Indium(III) Sensor based on a Thiosulfinate
503 Ionophore Derived from Omeprazole, *Bull. Korean Chem. Soc.* 34 (2013) 1153–1159.
504 doi:10.5012/bkcs.2013.34.4.1153.
- 505 [18] C. Pérez-Ràfols, N. Serrano, J.M. Díaz-Cruz, C. Ariño, M. Esteban, Simultaneous
506 determination of Tl(I) and In(III) using a voltammetric sensor array, *Sens. Actuators B*
507 *Chem.* 245 (2017) 18–24. doi:10.1016/j.snb.2017.01.089.
- 508 [19] J. Zhang, Y. Shan, J. Ma, L. Xie, X. Du, Simultaneous Determination of Indium and
509 Thallium Ions by Anodic Stripping Voltammetry Using Antimony Film Electrode, *Sens.*
510 *Lett.* 7 (2009) 605–608. doi:10.1166/sl.2009.1117.
- 511 [20] H. Sopa, L. Baldrianova, E. Tesarova, S.B. Hocevar, I. Svancara, B. Ogorevc, K. Vytras,
512 Insights into the simultaneous chronopotentiometric stripping measurement of
513 indium(III), thallium(I) and zinc(II) in acidic medium at the in situ prepared antimony film
514 carbon paste electrode, *Electrochimica Acta.* 55 (2010) 7929–7933.
515 doi:10.1016/j.electacta.2009.12.089.
- 516 [21] I. Geca, M. Korolczuk, Sensitive Anodic Stripping Voltammetric Determination of
517 Indium(III) Traces Following Double Deposition and Stripping Steps, *J. Electrochem.*
518 *Soc.* 164 (2017) H183–H187. doi:10.1149/2.0581704jes.
- 519 [22] K.C. Honeychurch, Recent Developments in the Stripping Voltammetric Determination
520 of Indium, *World J. Anal. Chem.* 1 (2013) 8–13. doi:10.12691/wjac-
521 1-1-2.

- 522 [23] J. Galceran, E. Companys, J. Puy, J. Cecilia, J.L. Garces, AGNES: a new electroanalytical
523 technique for measuring free metal ion concentration, *J. Electroanal. Chem.* 566 (2004)
524 95–109. doi:10.1016/j.jelechem.2003.11.017.
- 525 [24] R.F. Domingos, C. Huidobro, E. Companys, J. Galceran, J. Puy, J.P. Pinheiro, Comparison
526 of AGNES (absence of gradients and Nernstian equilibrium stripping) and SSCP (scanned
527 stripping chronopotentiometry) for trace metal speciation analysis, *J. Electroanal. Chem.*
528 617 (2008) 141–148. doi:10.1016/j.jelechem.2008.02.002.
- 529 [25] L.S. Rocha, E. Companys, J. Galceran, H.M. Carapuça, J.P. Pinheiro, Evaluation of thin
530 mercury film rotating disk electrode to perform absence of gradients and Nernstian
531 equilibrium stripping (AGNES) measurements, *Talanta*. 80 (2010) 1881–1887.
532 doi:10.1016/j.talanta.2009.10.038.
- 533 [26] M.H. Tehrani, E. Companys, A. Dago, J. Puy, J. Galceran, Free indium concentration
534 determined with AGNES, *Sci. Total Environ.* 612 (2018) 269–275.
535 doi:10.1016/j.scitotenv.2017.08.200.
- 536 [27] N. Serrano, J.M. Díaz-Cruz, C. Ariño, M. Esteban, Stripping Chronopotentiometry in
537 Environmental Analysis, *Electroanalysis*. 19 (2007) 2039–2049.
538 doi:10.1002/elan.200703956.
- 539 [28] R.M. Town, H.P. van Leeuwen, Effects of adsorption in stripping chronopotentiometric
540 metal speciation analysis, *J. Electroanal. Chem.* 523 (2002) 1–15. doi:10.1016/S0022-
541 0728(02)00747-7.
- 542 [29] E. Companys, J. Galceran, J.P. Pinheiro, J. Puy, P. Salaün, A review on electrochemical
543 methods for trace metal speciation in environmental media, *Curr. Opin. Electrochem.* 3
544 (2017) 144–162. doi:10.1016/j.coelec.2017.09.007.
- 545 [30] E.M. Thurman, R.L. Malcolm, Preparative isolation of aquatic humic substances, *Environ.*
546 *Sci. Technol.* 15 (1981) 463–466. doi:10.1021/es00086a012.
- 547 [31] W.G. Botero, M. Pineau, N. Janot, R.F. Domingos, J. Mariano, L.S. Rocha, J.E.
548 Groenenberg, M.F. Benedetti, J.P. Pinheiro, Isolation and purification treatments change
549 the metal-binding properties of humic acids: effect of HF/HCl treatment, *Environ. Chem.*
550 14 (2018) 417–424. doi:10.1071/EN17129.
- 551 [32] S.C.C. Monterroso, H.M. Carapuça, J.E.J. Simao, A.C. Duarte, Optimisation of mercury
552 film deposition on glassy carbon electrodes: evaluation of the combined effects of pH,
553 thiocyanate ion and deposition potential, *Anal. Chim. Acta.* 503 (2004) 203–212.
554 doi:10.1016/j.aca.2003.10.034.
- 555 [33] C. Parat, L. Authier, D. Aguilar, E. Companys, J. Puy, J. Galceran, M. Potin-Gautier,
556 Direct determination of free metal concentration by implementing stripping
557 chronopotentiometry as the second stage of AGNES, *Analyst*. 136 (2011) 4337–4343.
558 doi:10.1039/C1AN15481H.
- 559 [34] J.P. Gustafsson, Visual MINTEQ version 3.0. KTH, Department of Land and Water
560 Resources Engineering, Stockholm, Sweden, 2009. Available at <http://vminteq.lwr.kth.se/>,
561 (n.d.).
- 562 [35] E.A. Biryuk, V.A. Nazarenko, R.V. Ravitskaya, Spectrophotometric determination of the
563 hydrolysis constants of indium ions, *Russian Journal of Inorganic Chemistry*. 14 (1969)
564 503–506.
- 565 [36] W.W. Rudolph, D. Fischer, M.R. Tomney, C.C. Pye, Indium(III) hydration in aqueous
566 solutions of perchlorate, nitrate and sulfate. Raman and infrared spectroscopic studies and
567 ab-initio molecular orbital calculations of indium(III)–water clusters, *Phys. Chem. Chem.*
568 *Phys.* 6 (2004) 5145–5155. doi:10.1039/B407419J.
- 569 [37] F. Vydra, K. Štulík, E. Juláková, *Electrochemical stripping analysis.*, E. Horwood,
570 Chichester, 1976.

- 571 [38] C. Huidobro, E. Companys, J. Puy, J. Galceran, J.P. Pinheiro, The use of microelectrodes
572 with AGNES, *J. Electroanal. Chem.* 606 (2007) 134–140.
573 doi:10.1016/j.jelechem.2007.06.001.
- 574 [39] E. Rotureau, Analysis of metal speciation dynamics in clay minerals dispersion by
575 stripping chronopotentiometry techniques, *Colloids Surf. Physicochem. Eng. Asp.* 441
576 (2014) 291–297. doi:10.1016/j.colsurfa.2013.09.006.
- 577 [40] R.R. Nazmutdinov, T.T. Zinkicheva, G.A. Tsirlina, Z.V. Kuz'minova, Why does the
578 hydrolysis of In(III) aquacomplexes make them electrochemically more active?,
579 *Electrochimica Acta.* 50 (2005) 4888–4896. doi:10.1016/j.electacta.2005.02.091.
- 580 [41] J.M. Pingarron, R. Gallego-Andreu, P. Sanchez-Batanero, Potentiometric determination
581 of stability constants of complexes formed by Indium(III) and different chelating agents,
582 *Bull. Soc. Chim. Fr.* 3–4 (1984) 115–122.
- 583 [42] E. Vasca, D. Ferri, C. Manfredi, L. Torello, C. Fontanella, T. Caruso, S. Orrù, Complex
584 formation equilibria in the binary Zn²⁺–oxalate and In³⁺–oxalate systems, *Dalton Trans.*
585 0 (2003) 2698–2703. doi:10.1039/B303202G.
586